www.czasopisma.pan.pl PAN POLSKA AKADEMIA NAUK www.journals.pan.pl

Arch. Min. Sci. **69** (2024), 2, 231-251

Electronic version (in color) of this paper is available: http://mining.archives.pl

DOI: https://doi.org/10.24425/ams.2024.150343

VICTOR PATSON MUTAMBO[1*], SERHII CHUKHAREV[2], PARDON SINKALA[1], DRAIDA MIKOLONI[1]

THE INFLUENCE OF GEOTECHNICAL, GEOLOGICAL AND MINING FACTORS ON THE FORMATION OF SINKHOLES AT LUBAMBE MINE, ZAMBIA

Mining-induced sinkholes are a common feature in underground mines. Sinkholes usually disrupt mining operations and associated infrastructure when they occur. This paper presents a case study of the Lubambe copper mine, where nine (9) sinkholes have been reported on the eastern and southern limbs. The development of sinkholes has resulted in increased mining costs due to the closure of the 182 mL decline on the eastern limb and the 175 mL truck route on the southern limb.

This study establishes the influence that poor ground formation, rock stability, geological structures, and inappropriate mining practices have on the formation of surface sinkholes. Assessment of ground condition was done by core logging, and borehole analysis was conducted using GEM4D-BasRock software to classify the rock mass quality based on RQD, RMR, Q-System and GIS. Assessment of the mining operational environment was focused on the effects of varying stope designs and sequencing on ground stability. Results of the study indicate that the formation of surface-induced sinkholes is attributed to historical mining in weak rock formation and weathered rock coupled with subsequent failure of unsupported stopes with stope height between 8 and 25 metres and less stand-up time of 7 days.

Keywords: Surface-induced sinkholes; core logging; borehole analysis; rock mass quality

1. Introduction

Mining-induced sinkholes are common in underground mines. Their occurrences usually disrupt mining operations and associated infrastructure [1,2]. In mining areas, sinkholes can be caused by the application of mining methods that induce considerable ground displacements,

[1] UNIVERSITY OF ZAMBIA
[2] NATIONAL UNIVERSITY OF WATER AND NATURE, UKRAINE
* Corresponding author: vmutambo@unza.zm

such as block caving and mine dewatering activities. Besides disruption of mining activities, sinkholes also affect the water reticulation and electricity supply, causing damage to other mine-related infrastructure such as buildings and roads [3]. Therefore, mining-induced sinkholes are of major concern not only to the mining industry but also to relevant governments as regulators, environmental groups, and local communities in mine areas. Poonam and Lokhande [4] investigated the development and occurrences of sinkholes in Indian coal mines and concluded that most of the subsidence-induced sinkholes were attributed to mining depth, state of in-situ stresses, seam thickness, geological discontinuities, surface topography, dewatering activities, lowering of groundwater, rainfall, and earthquake. Nguyen Van Hoang et al. [5] established that most sinkholes develop within unconsolidated weathered rocks and dewatered mines. Sinkhole development can also be triggered by construction activities, excavation loading and drilling operations.

The work [6] noted that sinkhole development can lead to the collapse of excavation roofs and seepage of surface water into underground bedrock. Khanlari et al. [7] attributed the formation of sinkholes in the limestone of the western part of Iran to turbulent groundwater flow.

The work by [8-10] proposed a similar genetic classification of sinkholes. The work by [11] proposed a classification of sinkholes for evaporite karst areas. This text discusses the classification of sinkholes, which is similar to the classification presented in a previous study (reference [9]). In their study, Rupert and Spencer [12] identified three main types of sinkholes, namely collapse sinkholes, subsidence sinkholes, and solution sinkholes. According to this classification, solution sinkholes are formed due to the dissolution of bedrock joints caused by acidic water. This process which is gradual results in the formation of a bowl-shaped depression at the surface. On the other hand, subsidence sinkholes occur in areas where the overburden and bedrock are weak and non-cohesive [32]. Collapse sinkholes tend to develop without signs of depression at the surface until they finally collapse, leaving behind a deep hole. According to Rupert and Spencer [12], collapse sinkholes are the most dangerous, as they occur suddenly, and without any warning.

The majority of subsidence sinkholes developed in mining areas are due to both current and historical mining operations, which is common in Australia, Canada, the UK, France and Germany [13-19,31].

Identifications of geologic factors attributed to sinkhole development have been documented in different studies. Some of these studies have focused on the application of soil resistivity tomography and Ground penetrating radar (GPR) to map potential depressions attributed to sinkholes (Bekendam, 1998; Humnabadkar, 2022; Williams, 2003). Effects of the hydrogeological factors on sinkhole formation have also been widely established [13]. Similar work [20] investigated the impact of a sinkhole failure on groundwater contamination.

This study is aimed at investigating the influence of geotechnical, geological and mining factors on the formation of surface sinkholes using the Lubambe mine as a case study.

2. Lubambe Mine case study

2.1. Geographical location

Lubambe mine is located in the north-western extremity of the Zambian Copperbelt Province. It is approximately 468 Kkm from Lusaka. Fig. 1 shows the location of Lubambe Mine.

Fig. 1. Map of Zambia showing location of Lubambe Mine

2.2. Geological description

The Konkola North Copper deposit at Lubambe mine represents an autochthonous "Zambian-type" deposit within the late-Proterozoic Lufilian Arc fold and thrust belt. The deposit is hosted within sediments that accumulated in an intracratonic rift, which was subsequently closed during the Lufilian Orogeny.

The property is located in an area underlain largely by rocks belonging to the Katanga Sequence, Roan Group. This area is characterised by thick clastic sediments composed of predominantly arenaceous and argillaceous rocks with relatively thin interbeds of rudaceous material.

Copper mineralisation is largely hosted within the OS1 Member of the Nchanga Formation, the first major reducing horizon above a 1000 m-thick sequence of oxidised arkoses and conglomerates. The mineralised portion of the OS1 Member is usually between 15 and 20 m thick, and individual mines may have a strike length of over 10 km. At Lubambe Copper mine, the East and South limb orebody thickness ranges between 5 and 5.5 m. A complex paragenesis of Cu oxides and sulphides is present. Copper also occurs in its native form and within the lattice of metamorphic micas, i.e., the Chingola refractory ores. The OS1 Member siltstone unconformably overlies the Kafufya Formation and represents a sudden transgressive event. Although copper mineralisation occurs mostly within the OS1 Member, it is cross-cutting on a gross scale and pinches out towards the east within the overlying OS2 Member.

2.3. Mineralisation

Mineralisation occurs as finely disseminated sulphides assuming the grain size of the host rock, as coarser grains along bedding planes and cleavage, in thin veinlets, and lenticles and stringers. The sulphide minerals comprise chalcocite, chalcopyrite, bornite, digenite, covellite, pyrite and carrollite in approximate order of abundance. Non-sulphide copper minerals occur mainly along fractures and veins. The following are the main non-sulphide minerals which are observed in order of abundance: malachite, pseudo malachite, chrysocolla, cuprite, azurite and native copper. The assay hanging wall and footwall at the 1% T Cu cut-off grade are generally sharply defined. The results of the drilling programme indicate continuous mineralisation over an area of 28.2 km^2. A total geological resource, including Area 'A', of 297 M tonnes (Mt), at an average grade of 2.57% total Cu, is defined. Fig. 2 shows the stratigraphy of the deposit.

2.4. Mining methods

2.4.1. Historical mining and current mining method

Lubambe mine was previously mined in the 1950s, presumably using the room and pillar mining method, which left behind open stopes with rib pillars and interlevel sill pillars. From the voids left, this mining method exhibited a high degree of pillar robbing and also showed that production commenced quite close to the surface, as shown in Fig. 3, where some stopes were as close as 50 m to the surface, with the furthest at 140 m depth. The rib and sill pillars left were probably designed as crush pillars. Most of these pillars are assumed to have failed by now, considering that production was done over 70 years ago in the 1950s. The current mining method employed at Lubambe is longitudinal room and pillar. This method has a sequence of developing the main accesses and ore drives for the exploitation of the ore body. Once the ore drives are developed to the extremities, production commences by retreating from the limits of the ore drives towards the level of access. Fig. 4 shows the general mine layout of the Lubambe mine.

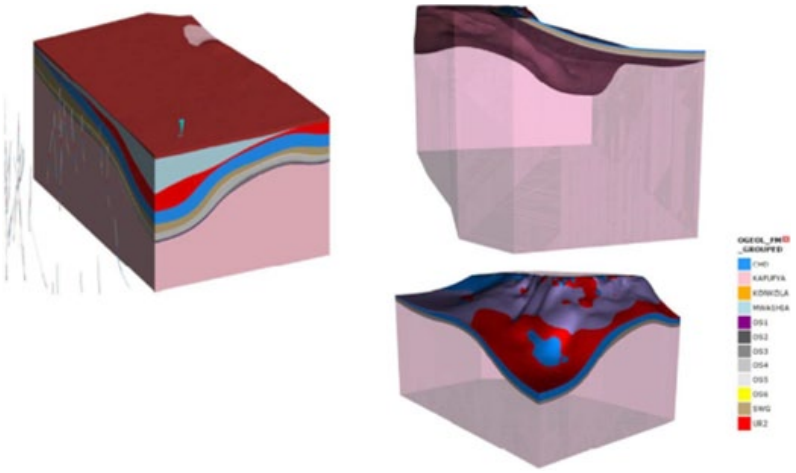

Fig. 2. Lubambe deposit stratigraphy

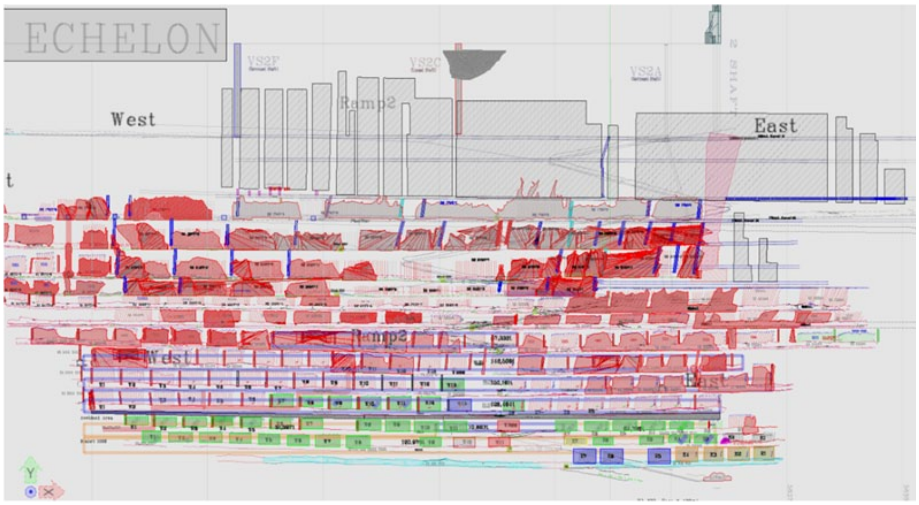

Fig. 3. Stopes from historical mining

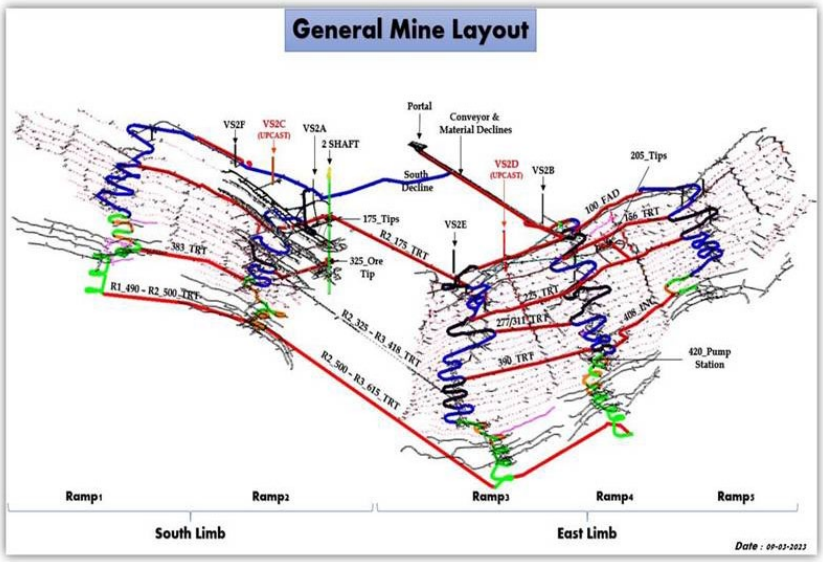

Fig. 4. Ramp 2 general mine lay out

2.4.2. Mining induced subsidence

Lubambe mine has, in the past 2 years (2020-2022), experienced a total of nine cases of subsidence that have resulted in the development of nine sinkholes on both the south and east limb caving areas of the mine [30]. The first-ever occurrence of subsidence at the mine was recorded on the 30th of May 2020 in the east limb caving area of the mine, as shown in Fig. 5.

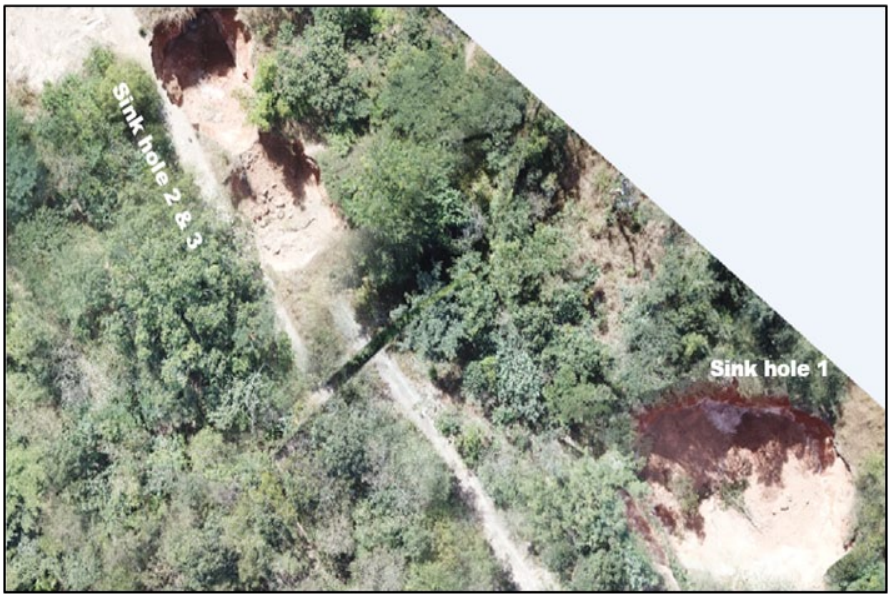

Fig. 5. East limb sinkholes

This incident resulted in the formation of three trough-shaped sinkholes. The total volumetric measurement of the ground that was subsidised was approximately 14,596 tonnes for all three sinkholes combined.

2.5. Lubambe geotechnical environment

2.5.1. Structural geology

The mean set plane for beddings is 48°/144° and the mean set plane for joints is 49°/227° while the mean set plane for the faults is 59°/284°. The structural joint set number is 3+R. The stereonet in Fig. 6 shows the mean joint sets for the south and east limb while the stereonet in Fig. 7 shows the brittle fault and preferential fault propagation for the whole mine.

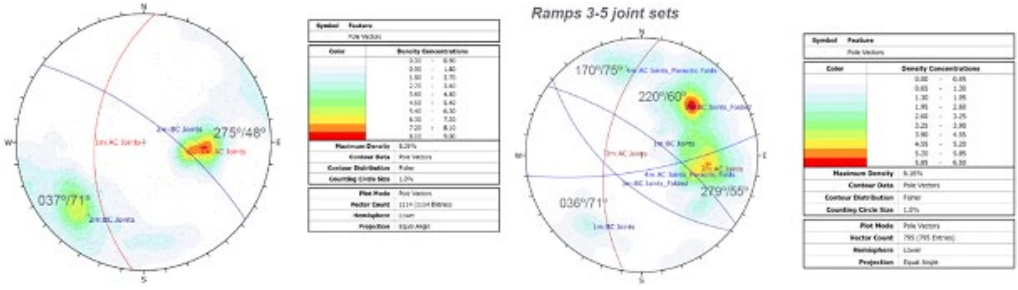

Fig. 6. Mean joint sets for the South and East limb

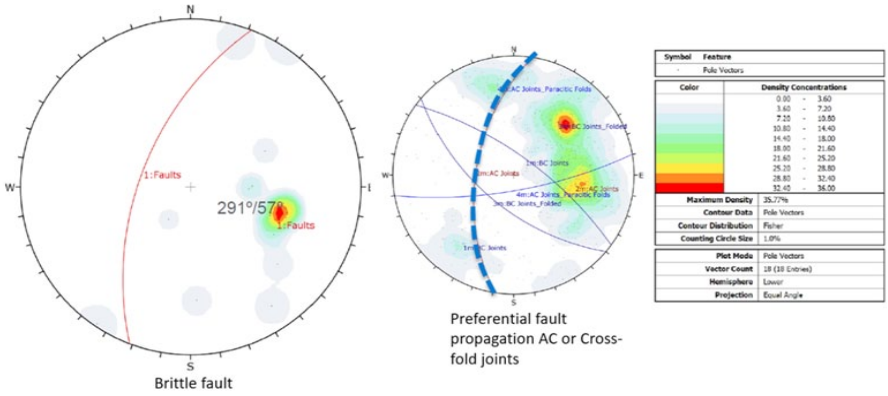

Fig. 7. Brittle fault and preferential fault propagation

2.5.2. Rock mass domains

A model of rock mass classification of the mine deposit using the rock quality designation (RQD) is presented in Fig. 8. Fig. 9 shows a model of the rock mass classification of the deposit using the Q-system. TABLE 1 summarises the geotechnical rock mass classification at

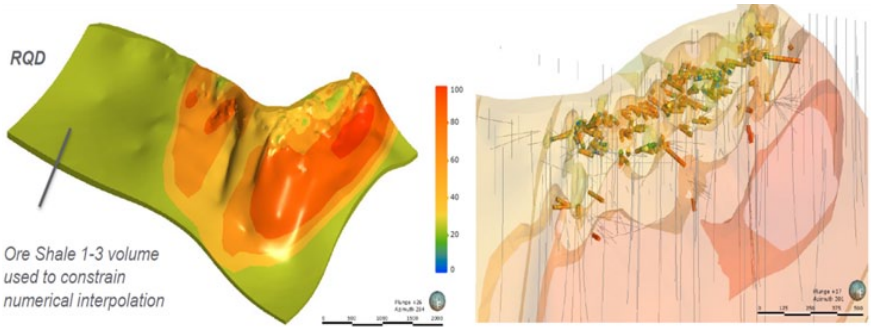

Fig. 8. Model of rock mass classification using the RQD for the Lubambe deposit

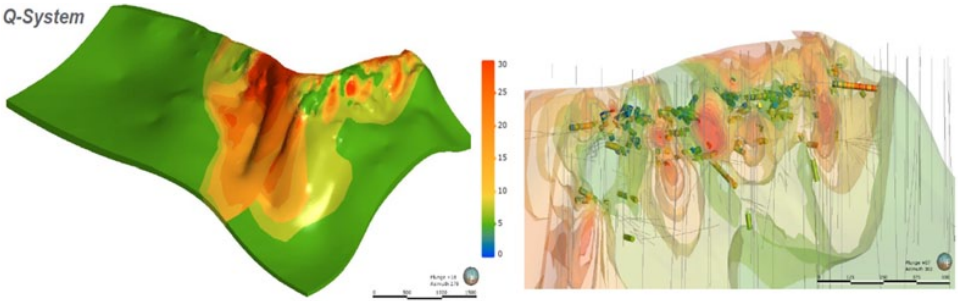

Fig. 9. Model of rock mass classification using the Q-System for the Lubambe deposit

TABLE 1

Geotechnical rock mass domains at Lubambe mine with median values

Domain by rock mass					
		Entire Mine	**FW**	**Ore Zone**	**HW**
RQD	25th Percentile	13	22	16	10
	Median	**34**	**45**	**37**	**30**
	75th Percentile	60	66.67	60	59
RMR	25th Percentile	51.30	10.00	53.27	49.19
	Median	**60.13**	**65.66**	**60.35**	**60.13**
	75th Percentile	67.56	72.60	66.85	68.73
Q	25th Percentile	2.25	4.63	2.8	1.78
	Median	**6**	**11.1**	**6.15**	**6**
	75th Percentile	13.7	24	12.67	15.6
Q'	25th Percentile	5.37	9.75	6.33	4.13
	Median	**14.25**	**21.89**	**13.88**	**13.17**
	75th Percentile	32.25	22.5	30	33

TABLE 2

Rock mass classification of footwall, orebody and hanging wall for five ramps in the entire mine

			Ramp 1						Ramp 2					
			FW		Ore Body		HW		FW		Ore Body		HW	
			AMC	SITE	AMC	SITE	AMC	SITE	AMC	SITE	AMC	SITE	AMC	SITE
Post 2018	RQD	Median	19	35	26	50	26	56	30	40	23	44	40	59
	RMR	Median	53.89	63.00	57.60	63.00	56.92	68.00	61.38	64.00	56.92	64.00	62.71	69.00
	Q	Median	3.00	16.12	4.53	14.86	4.2	25.8	6.9	16.61	4.2	16.3	8	27.8
	Q'	Median	7.5	40.3	11.33	37.16	10.5	64.6	17.25	41.52	10.5	40.8	20	69.6

			Ramp 3						Ramp 4					
			FW		Ore Body		HW		FW		Ore Body		HW	
			AMC	SITE	AMC	SITE	AMC	SITE	AMC	SITE	AMC	SITE	AMC	SITE
Post 2018	RQD	Median	38	45	22	57	48	64	18	48	30	60	32	67
	RMR	Median	62.13	65.00	53.89	68.00	61.38	70.00	64.356	66.000	68.005	68.000	63.775	71.000
	Q	Median	7.5	18.46	3	27.3	6.9	32.3	9.6	19.9	14.4	20.6	9	34.9
	Q'	Median	18.75	46.15	7.5	68.4	17.25	80.8	24	49.76	36	51.6	22.5	87.3

			Ramp 5					
			FW		Ore Body		HW	
			AMC	SITE	AMC	SITE	AMC	SITE
Post 2018	RQD	Median	42	34	40	58	40	53
	RMR	Median	60.85	63.00	60.13	64.00	60.98	67.00
	Q	Median	6.5	15.57	6	12.5	6.6	23.5
	Q'	Median	13.88	38.9	15	31.2	16.5	58.7

TABLE 3

Rock mass domain classification

Domain	Type
Domain 1	Arkose
Domain 2	Sand Stone
Domain 3	Lower Conglomerate
Domain 4	Ore Shale1
Domain 5	Ore Shale 2
Domain 6	Sand Zone
Domain 7	Kaolinite

Lubambe mine using RQD, rock mass rating (RMR), Q-System and Q techniques of rock mass classification, where the rock mass has been categorised into four groups namely; the entire mine, hanging wall, footwall and ore zone. TABLE 2 shows the rock mass classification of the ramp for the entire mine. The most commonly encountered geotechnical domains during the process of development and stopping at Lubambe mine are shown in TABLE 3.

The principal major domains affecting development design and/or stability are the sand zone (Domain 6) and the kaolinite (Domain 7), which are mostly unavoidable in Ramp 2 level access, and Ramp1 decline, which intercepts Domain 6 (sand zone). Ramps 5 and 3 intercept the kaolinite band approximately 10 m in width in the northern ore drives, while Ramps 1 and 2 intercept the band on the eastern and western ore drives in small traces. Furthermore, the traces are more prominent on the eastern side of the two Ramps.

2.5.3. Structures

Fig. 10 shows a 3-dimensional view of the dominant geological structures found at Lubambe mine. Two major geological structures have been mapped out and clearly defined as the sand zones and the faults. Two of the aforementioned structures exist in each of the limbs at the mine. The dominant band of sand on the south limb affects ramps 1 and 2, with one dominant fault cutting across ramp 2. On the east limb, the sand zone mostly affects ramps 4 and 5, while the major fault cuts across ramp 5 only.

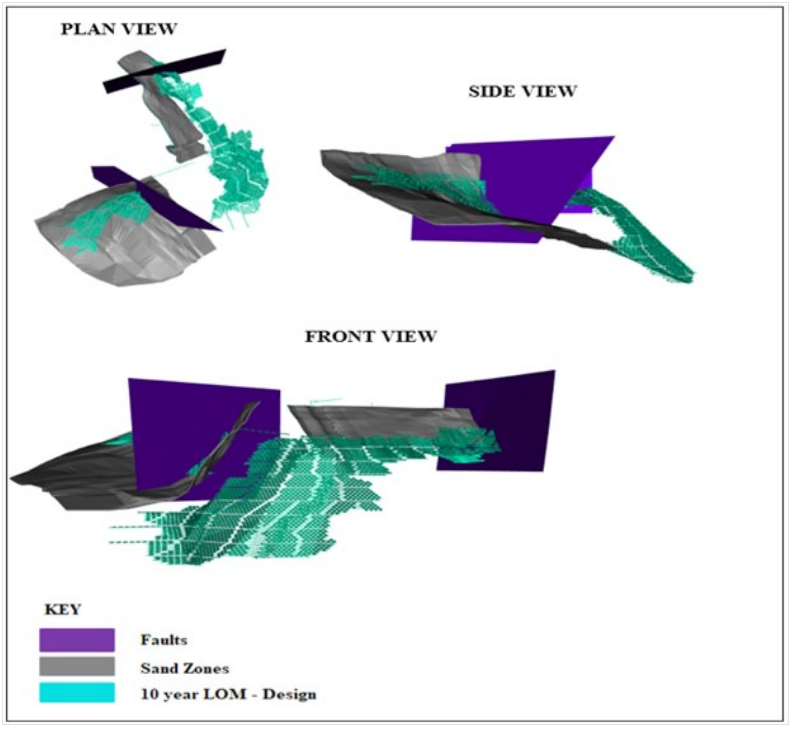

Fig. 10. Lubambe geological structures

3. Methodology

This study applied different methods and tools to assess the geotechnical, geological and mining environment.

Geotechnical logging was implemented at the Lubambe core shed, and existing data on rock mass characterisation was reviewed. Continuous diamond drilling was carried out by geology and geotechnical sections to understand rock mass and increase resource confidence.

After the core was logged, borehole analysis was conducted using GEM4D-BasRock software to classify the rock mass quality. To analyse the logged data, the following itemised steps were taken;

1. The string file of the borehole to be analysed was loaded in the GEM4D software. Thereafter, the string was split into 1m intervals and then saved.
2. Afterwards, a CSV file was created. The saved data was cleaned, followed by deleting the first row and the last 3 columns to ensure only the coordinates remained.
3. Then, the core logging database was opened, and four rock mass classification techniques were selected, namely; RQD, RMR, Q-System and GIS. The rock mass quality calculated for the four mentioned techniques was copied and pasted into the CSV file containing the string coordinates.
4. Finally, the file was saved and loaded into GEM4D for data visualisation and interpretation.

In addition, underground structural mapping was conducted to understand the discontinuities in the rock mass at Lubambe Mine. Thereafter, a kinematic analysis was carried out using the Rocscience software; DIPS and Unwedge to show the possible joint sets and possible wedges to be formed in the excavations. Data from the underground structural mapping was loaded into DIPS to obtain the mean joint sets, which were used to analyse the potentially unstable wedges around the excavations by Unwedge. The Rocscience software; RS3 which is a 3-dimensional analysis, and Phase 2D, which is a 2-dimensional software, were used for stress analysis. RS3 was used to display the string files of the sinkhole and show the areas of instability around the voids, while Phase 2D was used to show the stability of the hanging wall and footwall after progressive holing of four stopes on the east limb. Routine underground trips were undertaken across the mine to examine the current mining depth, characteristics of the host rock and orebody, average groundwater discharge per day, adherence to the stope designs, stand-up time, and mining and firing sequence during stope blasting.

4. Results and discussion

4.1. Borehole analysis

Borehole analysis using GEM4D, shown in Figs. 11-14, was conducted on four diamond-drilled boreholes in ramp 2_417mL on the south limb. The analysis on each borehole was conducted in 1m metre intervals in correlation with the core logging data, which was logged in the same intervals.

Rock quality designation (RQD) developed by [21] provides a quantitative estimate of rock mass quality from drilled cores (TABLE 4). RQD is defined as the percentage of intact core pieces longer than 100 mm (10 cm) in the total length of a core.

TABLE 4

RQD classification

Rock mass quality	RQD (%)
Very Poor	0-25
Poor	26-50
Fair	51-75
Good	76-90
Excellent	91-100

The average RQD for the borehole analysis was found to be 25.19% (Fig. 11). From the rock mass classification in TABLE 4, the RQD value of 25.19% falls under the poor rock mass category.

TABLE 5

RMR classification

Rating	100-81	80-61	60-41	40-21	<21
Class Number	I	II	III	IV	V
Description	Very good rock	Good rock	Fair rock	Poor rock	Very poor rock

Rock mass rating (RMR) by [22-24] classifies the rock mass using; the uniaxial compressive strength of rock material, rock quality designation, spacing of discontinuities, condition of discontinuities, groundwater conditions and orientation of discontinuities. The average RMR for the borehole analysis was found to be 49.71 (Fig. 12). From the classification in TABLE 5, the RMR rating of 49.71 implies that the rock mass quality is fair.

Q-system by [25] of the Norwegian Geotechnical Institute proposed a Tunneling Quality Index (Q) for the determination of rock mass characteristics and tunnel support requirements. The numerical value of the index Q varies on a logarithmic scale from 0.001 to a maximum of 1,000 and is defined by: Joint set number, Joint roughness, Joint alteration number, Joint water reduction factor and Stress reduction factor. The average Q-system for the borehole analysis was found to be 4.94, as shown in Fig. 13. From the rock mass classification that defines Q-system (TABLE 6), the rating of 4.94 falls under the category of fair rock mass quality.

TABLE 6

Q-System classification

Q-system	Rock Mass Quality
<1	Very poor
1.1-4	poor
4.1-10	Fair
10.1-40	Good
>40	Very good

The work by [26] introduced the GSI, for weak and hard rock medium. The average Geological strength index (GSI) value for the borehole analysis was found to be 44.71, as shown in Fig. 14. From the rock mass classification method that defines GSI, this rating falls under the category of fair rock mass quality.

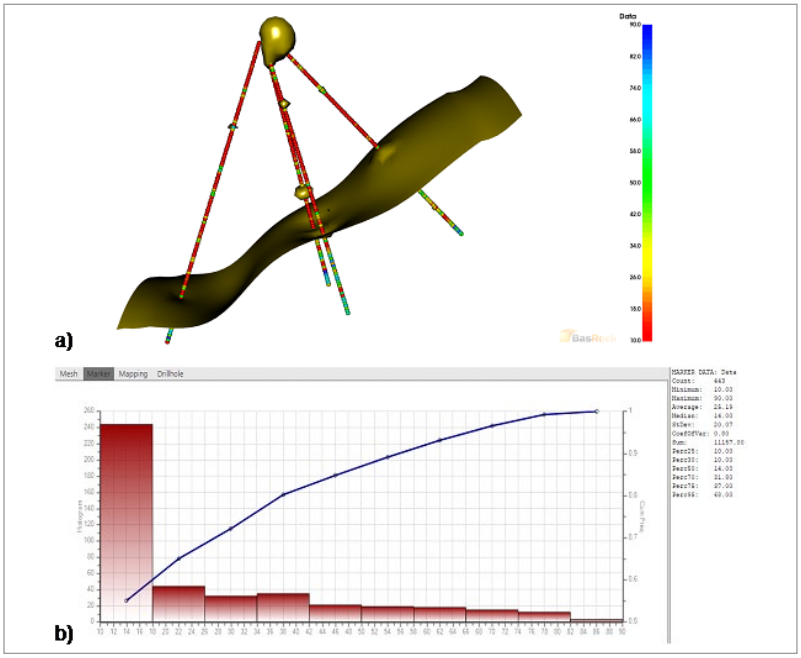

Fig. 11. RQD for ramp 2_417 mL, a) Borehole analysis, b) Data distribution

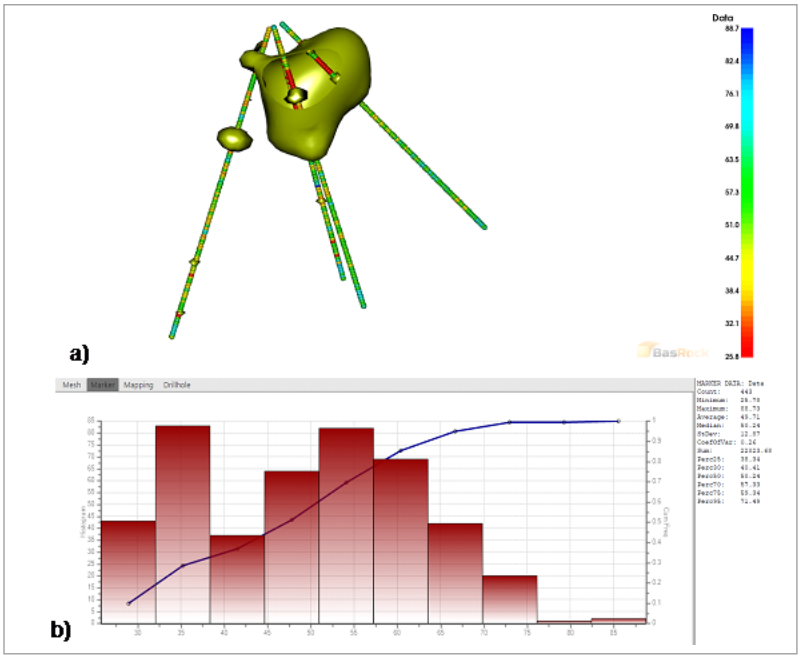

Fig. 12. RMR for ramp 2_417 mL, a) Borehole analysis, b) Data distribution

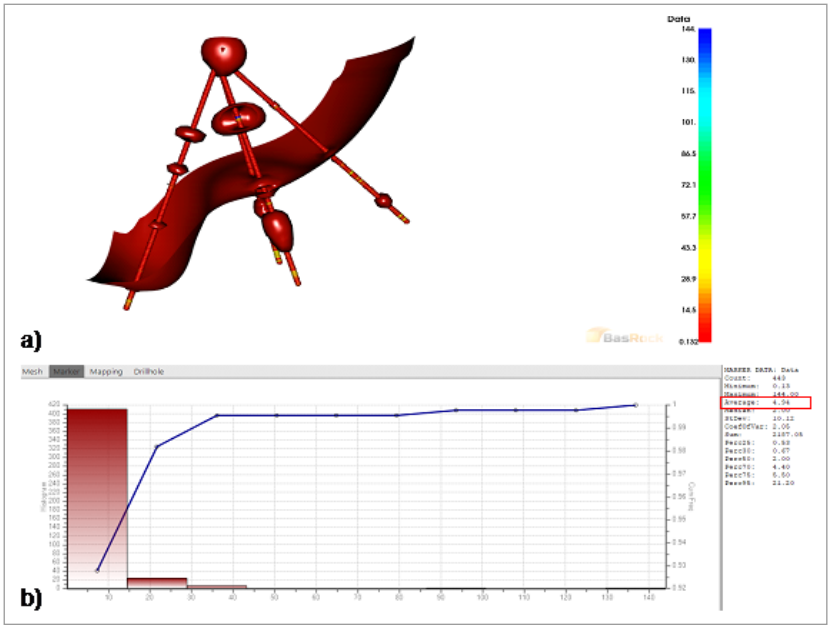

Fig. 13. Q-system for ramp 2_417 mL, a) Borehole analysis, b) Data distribution

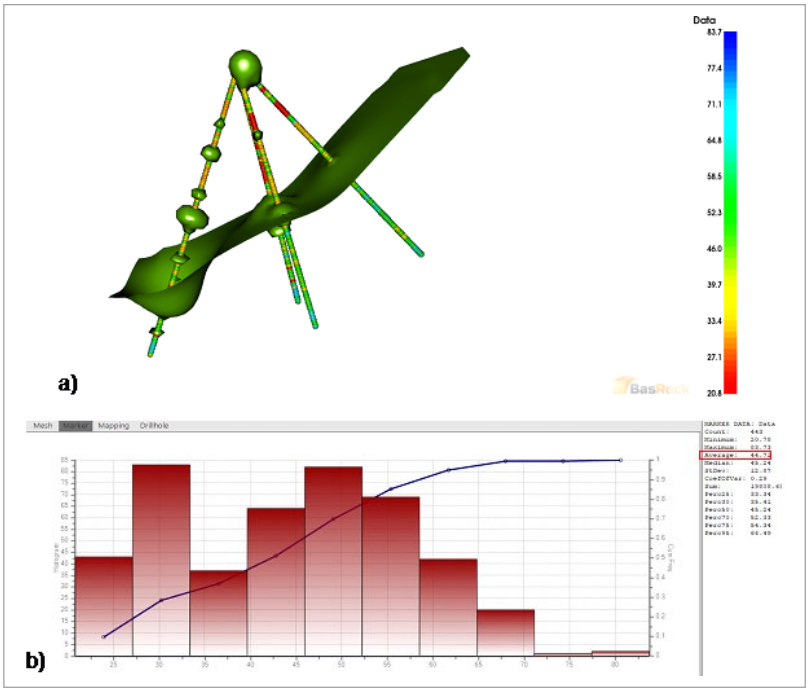

Fig. 14. GSI for ramp 2_417 mL, a) Borehole analysis, b) Data distribution

TABLE 7. Continued

4.2. Empirical borehole analysis

The RQD values in TABLE 7 show the rock mass quality of the ground condition from the south and east limbs separately. Empirical analysis of the rock mass classification using the RMR, Q-system and RQD results shows that the ground condition on the south and east limb can be classified as poor to fair (TABLE 8).

TABLE 7

Lubambe RQD values for different rock types in ramps 1,2,3,4 and 5

Ramp	Year	Rock Type	Ramp	RQD
1	2018 – 2022	Arkose	1	31%
	2018 – 2022	Shale	1	30%
	2018 – 2022	Conglomerate	1	27%
Average				**29%**
2	2018 – 2022	Arkose	2	31%
	2018 – 2022	Shale	2	31%
	2018 – 2022	Conglomerate	2	26%
Average				**29%**
3	2018 – 2022	Arkose	3	39%
	2018 – 2022	Shale	3	42%
	2018 – 2022	Conglomerate	3	38%
Average				**40%**
4	2018 – 2022	Arkose	4	48%
	2018 – 2022	Shale	4	38%
	2018 – 2022	Conglomerate	4	44%
Average				**43%**
5	2018 – 2022	Arkose	5	42%
	2018 - 2022	Shale	5	39%
	2018 – 2022	Conglomerate	5	41%
Average				**41%**

TABLE 8

South and east limb rock mass classifications based on RQD, RMR and Q-system

Limb	Criteria	Value	Classification
South	RQD	29%	Poor
	RMR	48.5%	Fair
	Q-System	3	Poor
East	RQD	41%	Poor
	RMR	51.2%	Fair
	Q-System	6.4	Fair

4.2.1. Stand-up time estimation using Rock Mass Rating

The ore drives at Lubambe mine are designed with dimensions of 5 m × 5 m, inclusive of permanent excavations mined for haulage, ventilation, dewatering, etc. These excavations are supported with welded mesh, split sets and face plates as the primary support system. The stopes on the other hand are left unsupported and have a varying stope height ranging between 8 and 25 metres that is dependent on the dip of the ore body. Based on the analysis from core logging, the RMR on the south and east limbs was 48.5% and 51.2%, respectively (TABLE 8). Fig. 15 shows that the expected stand-up time for an open stope at Lubambe Mine is 7 days. According to [27], stopes with arbitrary cross sections have higher chances of varying collapse mechanisms.

4.3. Structural mapping analysis

The Lubambe orebody dip varies from as low as 23° to about 89°. With the variation in the orebody dip, various failure modes are expected depending on the orientation and dip of the discontinuities in an area. Fig. 16 shows the mean joint sets at Lubambe Mine based on the structural mapping data that was collected underground. The analysis shows that there are three main joint sets plus one random joint (Fig. 16).

The two stereonets shown in Fig. 17 show the mean joint sets on the eastern and southern limbs of the mine. The east limb underground mapping data showed that there are 3 main joint sets plus 1 random joint, with the concentration of the joints located in the eastern hemisphere. The same case applies to the south limb, except that the concentration of the joints is in the western hemisphere.

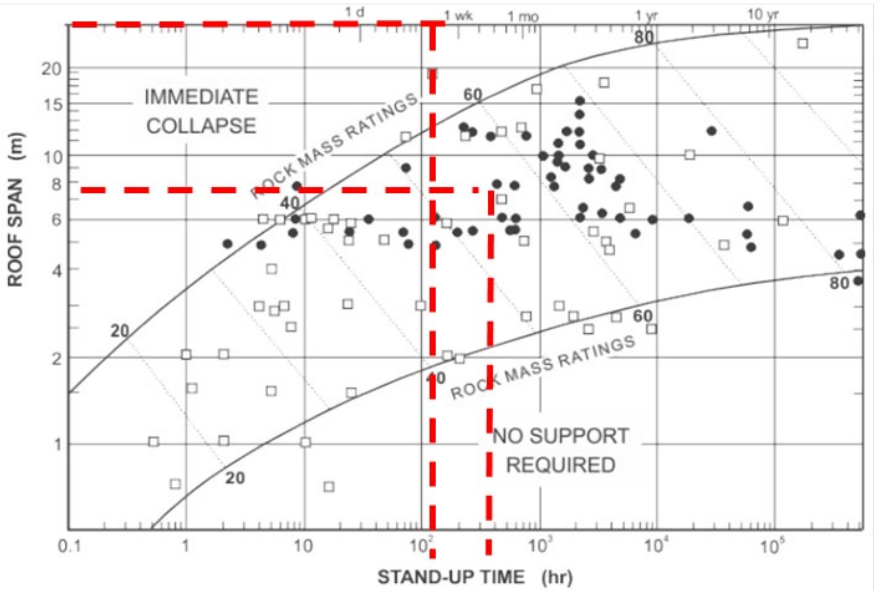

Fig. 15. RMR Stand-up time graph

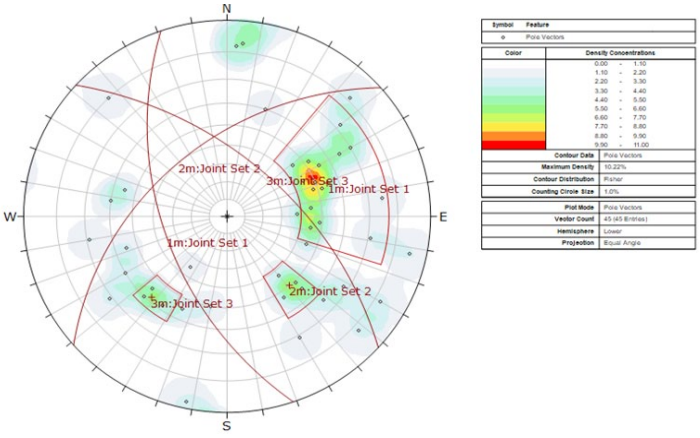

Fig. 16. Lubambe mean joint sets, obtained by DIPS software

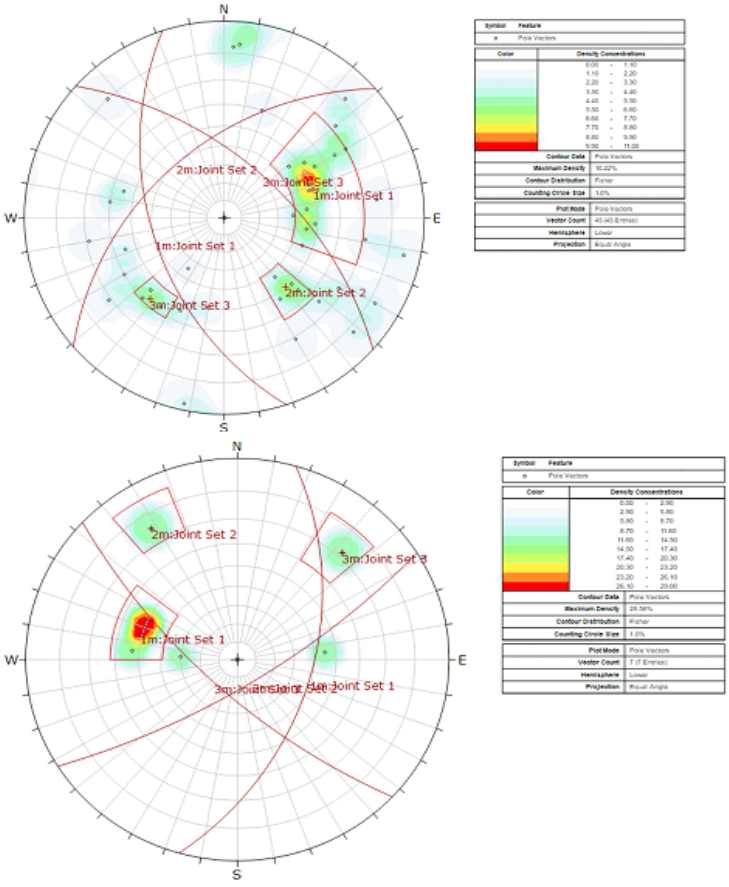

Fig. 17. East and South limb joint sets

Fig. 18 shows results from the kinematic analysis of the underground structural mapping data collected in the R4_524 south ore drive (SOD). The results show that wedges will form from the roof, floor, and excavation limits due to the interaction between joint sets and tunnel orientation, as shown on the stereonet.

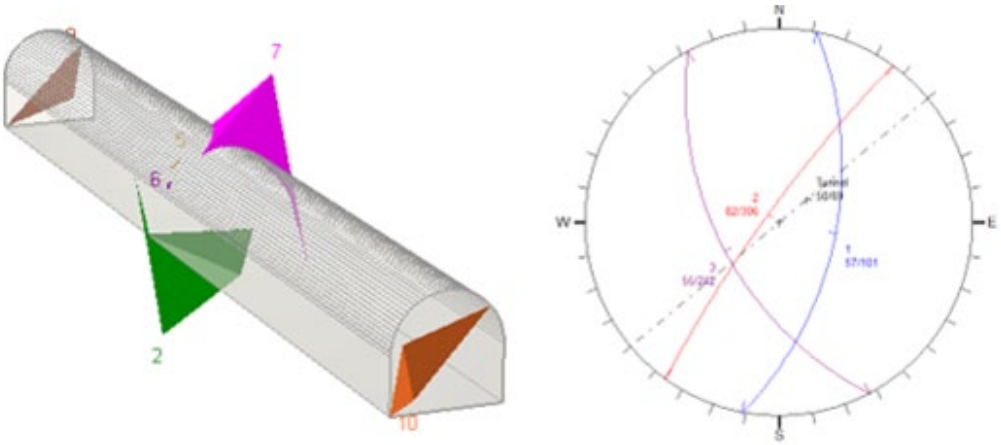

Fig. 18. Kinematic analysis of R4_524 SOD using Unwedge software

4.4. Assessment of mining operational environment

4.4.1. Stope design parameters

The Mathews-Potvin method [28,29] of assessing stope design parameters was applied. However, this method was only used as a guide in assessing the stope stability, because it is based on many assumptions, and the stability assessment was derived from a database based on experiences recorded from other operations. A high stability number and a low shape factor indicate a stable exposure, whilst a low stability number and a high shape factor indicate instability. It was observed that the performance of the ground at Lubambe appears to be significantly different from one limb to the other. Therefore, frequent investigation and planning for the hanging wall structure were seen as the most effective means of maintaining stope stability at Lubambe, as shown in Figs. 18-20 and TABLE 9, respectively.

4.4.2. Optimal stope spans

The geotechnical recommendation for all the ramps is the application of a 30 m stope, which is a stope span from rib to rib plus rib pillar. Hence, the stope span shall be calculated by subtracting 30 m – rib pillar length depending on mining depth. The current deepest mining depth at Lubambe is 574 mL from the surface; therefore the rib pillar dimensions in use are 6 m long pillars. Therefore, the current stope span is; 30 m – 6 m = 24 m.

		Q'	N'	Unsupported alowed HR (m)	Supported allowed HR (m)	Unsupported allowed L (m) 15	20	25	30	Supported allowed L (m) 15	20	25	30
25% Percentile	HW	7.2	2.10	3.1	7.8	10.7	9.1	8.3	7.9	>50	>50	41.5	32.5
	FW	5.7	3.22	3.6	8.5	14.2	11.5	10.3	9.6	>50	>50	>50	38.8
	Sidewall	6.2	5.08	4.3	9.2	20.4	15.2	13.2	12.1	>50	>50	>50	47.8
						Unsupported allowed L (m) 4	5	6	Supported allowed L (m) 4	5	6		
	Crown	6.2	3.41	3.7	8.5	>50	>50	>50	>50	>50	>50		
Median		Q'	N'	Unsupported alowed HR (m)	Supported allowed HR (m)	Unsupported allowed L (m) 15	20	25	30	Supported allowed L (m) 15	20	25	30
	HW	16.5	4.84	4.2	9.1	19.6	14.8	12.9	11.8	>50	>50	>50	46.7
	FW	13.9	7.88	5.1	10.0	31.6	20.7	17.2	15.4	>50	>50	>50	>50
	Sidewall	15.0	12.36	6.0	10.9	>50	30.1	23.1	20.1	>50	>50	>50	>50
						Unsupported allowed L (m) 4	5	6	Supported allowed L (m) 4	5	6		
	Crown	15.0	8.29	5.2	10.1	>50	>50	>50	>50	>50	>50		
75% Percentile		Q'	N'	Unsupported alowed HR (m)	Supported allowed HR (m)	Unsupported allowed L (m) 15	20	25	30	Supported allowed L (m) 15	20	25	30
	HW	30.0	8.81	5.3	10.2	36.1	22.6	18.4	16.4	>50	>50	>50	>50
	FW	29.6	16.83	6.7	11.6	>50	41.3	29.2	24.5	>50	>50	>50	>50
	Sidewall	28.1	23.18	7.6	12.3	>50	>50	38.6	30.7	>50	>50	>50	>50
						Unsupported allowed L (m) 4	5	6	Supported allowed L (m) 4	5	6		
	Crown	28.1	15.55	6.5	11.4	>50	>50	>50	>50	>50	>50		

Fig. 19. Stope design parameters for allowable unsupported Hydraulic Radius – HR (m)

Fig. 20. Stope design parameters for ramps

TABLE 9

Post stope stability Ramp showing changes in factor of safety (FOS) with increase in depth and pillar size

Depth (m)	Pillar width(m)	450m	550m	650m	750m	850m	950m	1050m
450	4	0.8	0.7	0.6	0.5	0.4	0.4	0.3
550	5	1.1	0.9	0.8	0.7	0.6	0.5	0.5
650	6	1.5	1.2	1.0	0.9	0.8	0.7	0.6
750	7	1.9	1.5	1.3	1.1	1.0	0.9	0.8
850	8	2.2	1.8	1.5	1.3	1.2	1.0	0.9
950	9	2.6	2.1	1.8	1.6	1.4	1.2	1.1
1050	10	3.0	2.4	2.1	1.8	1.6	1.4	1.4

KEY		
0.0 <FoS<	1.3	
1.30 <=FoS<	1.5	
1.50 <=FoS		

5. Conclusion

This study sought to establish the influence that the geotechnical, geological and mine operational environment has on induced sinkholes at the Lubambe copper mine. From the study undertaken, mining-induced sinkholes are due to:

1. There are both historical and current mining operations in the area. The historical method involved room and pillar mining in poor rock formations near the surface. The current method is used at greater depths with better rock formations and has a shorter stand-up time of 7 days. Information from historical mining conducted in the 1950s shows that production at Lubambe started on the southern limb at 100 mL, some of the stopes were as close as approximately 54 m from the surface and very unstable. Room and pillar require that adjustment of stope parameters be undertaken with an increase in stresses and mine depth.
2. The results from both numerical and empirical analysis show a correlation in the results obtained, indicating that the ground condition at the mine at the current mining depth of 574 mL can be classified as poor to fair. Furthermore, the visual assessment conducted across the mine corresponded with the analysis done.
3. Geotechnical analysis by numerical modelling showed that the surface subsidence occurred as a result of progressive holing of stopes in ramp 3 between 113 mL and 165 mL, where a huge void was formed in the highly weathered rock mass. This led to the caving in of the hanging wall, which propagated to the surface as subsidence. The excess material that accumulated underground caused the overloading of the pillar at 182 mL decline, which was mined close to the ore drive, thereby triggering the failure of the decline as a result of pillar failure.
4. With the increase in mining depth, currently at 574 mL, the mine will not anticipate subsidence-induced sinkholes due to changes in rock formation, which can be classified as fair, and the pending transition to post-fill room and pillar mining method.

Acknowledgment

We would like to extend our sincere gratitude to Lubambe Copper Mine for allowing this study to be undertaken at the mine. All the members of staff at the mine were very helpful during data collection and consultation at every level throughout the research study.

References

[1] A.H. Cooper, A.C. Waltham, Subsidence caused by gypsum dissolution at Ripon, North Yorkshire. Quarterly Journal of Engineering Geology and Hydrogeology **32** (4), 305-310 (1999). DOI: https://doi.org/10.1144/GSL.QJEG.1999.032.P4.01

[2] F. Gutiérrez, A.H. Cooper, Evaporite dissolution subsidence in the historical city of Calatayud, Spain: damage appraisal and prevention. Natural Hazards **25**, 259-288 (2002). DOI: https://doi.org/10.1023/A:1014807901461

[3] A. Humnabadkar, Preventing Sinkholes in Mining: Recent Development in the Industry. Available at: https://www.azomining.com/Article.aspx?ArticleID=1696. Accessed: 05/03/2023

[4] P. Sahu, R.D. Lokhande, An Investigation of Sinkhole Subsidence and its Preventive Measures in Underground Coal Mining. Procedia Earth and Planetary Science **11**, 63-75 (2015). DOI: https://doi.org/10.1016/j.proeps.2015.06.009

[5] N.V. Hoang, H.V. Hung, T.Q. Cuong, Characteristics and Affecting Factors of Sinkhole Development in Cho Don Area, Bac Kan Province, Vietnam. IOP Conf. Ser.: Earth Environ. Sci. 690012025. DOI: https://doi.org/10.1088/1755-1315/690/1/012025

[6] G. Newton, Development of sinkholes resulting from man's activities in the Eastern United States. Circular 968, Report, USA. DOI: https://doi.org/10.3133/cir968

[7] G.R. Khanlari, H. Mojtaba, A.A. Momeni, A. Mohemed, A.T. Beydokhti, The effect of groundwater overexploitation on land subsidence and sinkhole occurrences, West of Iran. Quarterly J. of Eng. Geo. and Hydrogeo **45** (4), 447-456 (2012). DOI: https://doi.org/10.1144/qjegh2010-069

[8] P. Williams, Dolines. In: Gunn J. (ed.) Encyclopedia of caves and karst science, Fitzroy Dearborn, New York, pp. 304-31 (2003).

[9] B.F. Beck, Soil piping and sinkhole failures. In: White WB (ed.) Encyclopedia of Caves. Elsevier: New York, pp. 523-528 (2004).

[10] T. Waltham, F. Bell, M. Culshaw, Sinkholes and subsidence: Karst and Cavernous Rocks in Engineering and Construction. Springer Berlin, Heidelberg, 382 pp, (2005).

[11] F. Gutiérrez, A.H. Cooper, K.S. Johnson, Identification, prediction and mitigation of sinkhole hazards in evaporite karst areas. Environmental Geology **53**, 1007-1022 (2008). DOI: https://doi.org/10.1007/s00254-007-0728-4

[12] F. Rupert, S. Spencer, Florida Sinkholes. Florida Geological Survey, Poster 11. Florida Geological Survey, Florida Department of Environmental Protection, Tallahassee, Florida. (2004). Accessed 07/06/2023. Availableat: https://aquadocs.org/bitstream/handle/1834/18557/Poster11.pdf?sequence=1&isAllowed=y

[13] F.S. Ebrahim, A numerical investigation of the mechanisms of post-mining subsidence. PhD Thesis, The University of Newcastle, Australia (2016). Available at https://nova.newcastle.edu.au/vital/access/%20/manager/Repository/uon:27428?view=null&f. Accessed: 15/12/2022.

[14] A.C Waltham, G.M. Swift, Bearing capacity of rock over mined cavities in Nottingham. Engineering Geology **75**, 15-31 (2004). DOI: http://dx.doi.org/10.1016/j.enggeo.2004.04.006

[15] J. Taylor, R. Fowell, Statistical associations concerning the life of coal pillars. Proceedings of the Post-Mining 2008, Nancy, 1-7 (2008)

[16] R.F. Bekendam, Pillar stability and large-scale collapse of abandoned limestone room and pillar mines in South-Limburg, The Netherlands, PhD-thesis TU Delft (1998). Available at: http://resolver.tudelft.nl/uuid:bfe483a5-312e-4213-ab45-1e75a147b1f2. Accessed 06/05/2023

[17] C. Didier, The French experience of post-mining management. Symposium Post-Mining 2008. ASGA. Vandoeuvre-lès-Nancy, NC (2008).

[18] C. Didier, R. Salmon, Assessment of the risk of a sinkhole appearing on a surface: A probabilistic volumetric model. National days of Geotechnics and Geology, Lile, France, pp. 441-451 (2004). Available at: https://ineris.hal.science/ineris-00972467/document. Accessed on 17/04/2023

[19] G. Swift, D. Reddish, Stability problems associated with an abandoned ironstone mine. Bull. Eng. Geol. Environ. **61**, 227-239 (2002). DOI: https://doi.org/10.1007/s10064-001-0147-9

[20] D. Sandhu, Implications of Groundwater Plume Transport and Analysis of Karst Aquifer Characteristics in Central Florida. (2019). Electronic Theses and Dissertations. 6575 (2019). Available at: https://stars.library.ucf.edu/etd/6575. Accessed:30/04/2023

[21] D.U. Deere, D.W. Miller, The Rock Quality Designation (RQD) Index in Practice, Classification Systems for Engineering Purposes. ASTM STP, American Society for Testing and Materials, Philadelphia, PA, 91-101 (1967). DOI: https://doi.org/10.1520/STP48465S

[22] Z.T. Bieniawski, Rock mass classification in rock engineering. In: Bieniawski, Z.T. (Ed.), Exploration for Rock Engineering, Proceedings of the Symposium **1**. Balkema, Cape Town, pp. 97-106 (1976).

[23] Z.T. Beniawaski, Rock Mechanics Design in Mining and Tunneling. A.A. Balkema, 274 (1984).

[24] Z.T. Bieniawski, Engineering rock mass classifications. New York: Wiley, (1989).

[25] N. Barton, R. Lien, J. Lunde, Engineering classification of Rock Masses for the design of Tunnel support. Rock Mechanic **6**, 189-236, Springer (1974).

[26] E. Hoek, E.T. Brown, Practical Estimates of Rock Mass Strength. International Journal Rock Mechanics Mining Science **34**, 1165-1186 (1997).

[27] M. Fraldi, F. Guarracino, Analytical solutions for collapse mechanisms in tunnels with arbitrary cross sections. International Journal of Solids and Structures **47** (2), 216-223 (2010). DOI: https://doi.org/10.1016/j.ijsolstr.2009.09.028

[28] K.E. Mathews, E Hoek, D.C. Wyllie, S. Stewart, Prediction of stable excavation spans for mining at depths below 1000 m in hard rock. CANMET DSS Serial No: 0sQ80-00081. Ottawa, (1981).

[29] Y. Potvin, Empirical open stope design in Canada. PhD thesis, University of British Columbia, Canada (1988)

[30] V. Mutambo, D. Mikoloni, Investing the causes and effects of mining induced subsidence due to sinkholes on the southern and eastern limb at Lubambe mine. in: Prospects for developing resource-saving technologies in mineral mining and technologies. Multi-authored monograph – Petrosani, Romania. UNIVERSITETAS publishing, 94-109 (2022). DOI: https://doi.org/10.31713/m1105

[31] T. Waltham, Sinkhole Geo-hazards, Geology Today **25** (3), 112-116 (2009).

[32] J. Guerrero, F. Gutiérrez, P. Lucha, The impact of halite dissolution subsidence on fluvial terrace development.: The case study of the Huerva River in the Ebro Basin (NE Spain). Geomorphology **100** (1-2), 64-179 (2008). DOI: https://doi.org/10.1016/j.geomorph.2007.04.040